Inorg. Chem. **2006**, *45*, 8608–8617

New Ruthenium Nitrosyl Complexes with Tris(1-pyrazolyl)methane (tpm) and 2,2′-Bipyridine (bpy) Coligands. Structure, Spectroscopy, and Electrophilic and Nucleophilic Reactivities of Bound Nitrosyl

Mariela Videla,[†] Julián S. Jacinto,[†] Ricardo Baggio,[‡] María T. Garland,[§] Priti Singh,[||] Wolfgang Kaim,[||] Leonardo D. Slep,[†] and José A. Olabe*,[†]

Department of Inorganic, Analytical and Physical Chemistry and INQUIMAE, CONICET, Facultad de Ciencias Exactas y Naturales, Universidad de Buenos Aires, Pabellón 2, Ciudad Universitaria, C1428EHA Buenos Aires, Argentina, Department of Physics, Comisión Nacional de Energía Atómica, Centro Atómico Constituyentes, Avenida Gral. Paz 1499, San Martín B1650KNA, Prov. de Buenos Aires, Argentina, Department of Physics, Facultad de Ciencias Físico Matemáticas, Universidad de Chile, and CIMAT, Avenida Blanco Encalada 2008, Santiago, Chile, and Institut fuer Anorganische Chemie, Universität Stuttgart, Pfaffenwaldring 55, D-70550 Stuttgart, Germany

Received June 13, 2006

The new compound $[Ru(bpy)(tpm)NO](ClO_4)_3$ [tpm = tris(1-pyrazolyl)methane; bpy = 2,2′-bipyridine] has been prepared in a stepwise procedure that involves the conversion of $[Ru(bpy)(tpm)Cl]^+$ into the aqua and nitro intermediates, followed by acidification. The diamagnetic complex crystallizes to exhibit distorted octahedral geometry around the metal, with the Ru–N(O) bond length 1.774(12) Å and the RuNO angle 179.1(12)°, typical for a $\{RuNO\}^6$ description. The $[Ru(bpy)(tpm)NO]^{3+}$ ion (**I**) has been characterized by ^1H NMR and IR spectroscopies (ν_{NO} = 1959 cm^{-1}) and through density functional theory calculations. Intense electronic transitions in the 300–350-nm region are assigned through time-dependent (TD)DFT as intraligand $\pi \rightarrow \pi^*$ for bpy and tpm. The $d\pi \rightarrow \pi^*$(bpy) metal-to-ligand charge-transfer transitions appear at higher energies. Aqueous cyclic voltammetric studies show a reversible wave at 0.31 V (vs Ag/AgCl, 3 M Cl^-), which shifts to 0.60 V in MeCN, along with the onset of a wave of an irreversible process at –0.2 V. The waves are assigned to the one- and two-electron reductions centered at the NO ligand, leading to species with $\{RuNO\}^7$ and $\{RuNO\}^8$ configurations, respectively. Controlled potential reduction of **I** in MeCN led to the $[Ru(bpy)(tpm)NO]^{2+}$ ion (**II**), revealing a significant downward shift of ν_{NO} to 1660 cm^{-1} as well as changes in the electronic absorption bands. **II** was also characterized by electron paramagnetic resonance, showing an anisotropic signal at 110 K that arises from an $S = {}^1/_2$ electronic ground state; the *g*-matrix components and hyperfine coupling tensor resemble the behavior of related $\{RuNO\}^7$ complexes. Both **I** and **II** were characterized through their main reactivity modes, electrophilic and nucleophilic, respectively. The addition of OH^- into **I** generated the nitro complex, with $k_{OH} = 3.05 \times 10^6$ M^{-1} s^{-1} (25 °C). This value is among the highest obtained for related nitrosyl complexes and correlates with $E_{NO^+/NO}$, the one-electron redox potential. Complex **II** is a robust species toward NO release, although a conversion to **I** was observed in the presence of O_2. This reaction afforded a second-order rate law with k = 3.5 M^{-1} s^{-1} (25 °C). The stabilization of the NO radical complex is attributed to the high positive charge of the precursor and to the geometrical and electronic structure as determined by the neutral tpm ligand.

Introduction

Nitrogen monoxide, NO, exhibits many physiological roles such as blood pressure control, neurotransmission, and immune response against microorganisms and tumors.[1] This small molecule is known to interact with transition-metal ions in biological fluids, though the understanding of the detailed

* To whom correspondence should be addressed. E-mail: olabe@qi.fcen.uba.ar.
[†] Universidad de Buenos Aires.
[‡] Comisión Nacional de Energía Atomica.
[§] Universidad de Chile.
[||] Universität Stuttgart.

(1) (a) Feelisch, M., Stamler, J. S., Eds.; *Methods in Nitric Oxide Research*; Wiley: Chichester, U.K., 1996. (b) Ignarro, J. L. E. *Nitric Oxide, Biology and Pathobiology*; Academic Press: San Diego, CA, 2000. (c) Butler, A. R.; Megson, I. L. *Chem. Rev.* **2002**, *102*, 1155−1165. (d) Beckman, J. S. The Physiological and Pathological Chemistry of Nitric Oxide. In *Nitric Oxide, Principles and Actions*; Lancaster, J., Ed.; Academic Press: San Diego, CA, 1996.

10.1021/ic061062e CCC: $33.50
Published on Web 09/09/2006

mechanisms implicated in many biorelevant processes is still incomplete. There is thus persistent interest in basic studies on the coordination chemistry of NO that points toward an improvement of our knowledge about these processes.[2]

Metal nitrosyl complexes have been known for a long time, leading to a considerable number of well-characterized $[ML_xNO]$ compounds that span different coordination numbers.[3,4] Enemark and Feltham (E−F) have *early* shown that the overall structural and reactivity features of these metal nitrosyls can be rationalized in terms of their $\{MNO\}^n$ description, where n is the sum of metal d electrons and the nitrosyl π^* electrons.[5] Many of these well-studied species correspond to $n = 6$, with linear MNO arrangements and an electrophilic reactivity centered at the N atom of the MNO moiety. Bent MNO bonds have been found for species with $n = 7$ and 8, which also display a shift to nucleophilic reactivity.[5−7] The E−F description avoids any mention of the *identity* of L, which roughly does not appreciably effect the *geometrical* features within the different complexes of a given $\{MNO\}^n$ configuration. However, L may exert a significant influence on the spectroscopic and reactivity properties, determining the values of the IR stretching frequencies, ν_{NO}, and/or the redox potentials of the metal-lonitrosyl couples, $E_{NO^+/NO}$.[8,9]

Some of the most systematically studied nitrosyl complexes involve group 8 metals, with emphasis on Ru, in conjunction with a variety of coligands (NH_3, H_2O, CN^-, ethylenediaminetetraacetic acid, polypyridines, porphyrins, etc.).[8−10] Despite the large amount of well-described species, an effort has been made in recent years to prepare new six- and five-coordinated $\{RuNO\}^6$ molecules, by introducing selected coligands L in the coordination sphere.[11,12] The basic *structural* aspects predicted by the E−F formalism have been confirmed. However, the studies on the electrophilic reactivities of some of these complexes[12] merit a critical discussion, as will be shown here.

To prepare new $\{RuNO\}^{6,7}$ species, we revisit the tris(1-pyrazolyl)methane (tpm) chemistry.[13−15] This tridentate ligand is a member of the family of "scorpionate" molecules[13,16] and binds Ru in the *fac* configuration. It has been described as a σ donor and weak π donor/acceptor. The coordination sphere of Ru is completed with a 2,2′-bipyridine (bpy) molecule. We report here on the preparation, crystal structure, spectroscopy, and electrophilic reactivity of the $\{RuNO\}^6$ complex $[Ru(bpy)(tpm)NO](ClO_4)_3$. Through one-electron reduction of solutions of the $[Ru(bpy)(tpm)NO]^{3+}$ ion (**I**), we also describe the related $\{RuNO\}^7$ species $[Ru(bpy)(tpm)NO]^{2+}$ (**II**). Although the structural and spectroscopic characterization of complexes with $n = 7$ has been attained in recent years,[17] reactivity properties still remain poorly investigated.[2] We explore the reaction with O_2, a study

(2) (a) Ford, P. C.; Lorkovic, I. M. *Chem. Rev.* **2002**, *102*, 993−1017. (b) Ford, P. C.; Laverman, L.; Lorkovic, I. *Adv. Inorg. Chem.* **2003**, *54*, 203−257. (c) Lim, M. D.; Lorkovic, I.; Ford, P. C. *J. Inorg. Biochem.* **2005**, *99*, 151−165. (d) Ford, P. C.; Laverman, L. E. *Coord. Chem. Rev.* **2005**, *249*, 391−403. (e) McCleverty, J. A. *Chem. Rev.* **2004**, *104*, 403−418.

(3) Richter-Addo, G. B.; Legzdins, P. *Metal Nitrosyls*; Oxford University Press: New York, 1992.

(4) Olabe, J. A.; Slep, L. D. Reactivity and Structure of Complexes of Small Molecules: Nitric and Nitrous Oxide. In *Comprehensive Coordination Chemistry II, from Biology to Nanotechnology*; McCleverty, J. A., Meyer, T. J., Eds.; Elsevier: Oxford, U.K., 2004; Vol. 1, pp 603−623.

(5) Enemark, J. H.; Feltham, R. D. *Coord. Chem. Rev.* **1974**, *13*, 339−406.

(6) (a) Westcott, B. L.; Enemark, J. H. Transition Metal Nitrosyls. In *Inorganic Electronic Structure and Spectroscopy*; Solomon, E. I., Lever, A. B. P., Eds.; Wiley: New York, 1999; Vol. II, pp 403−450. (b) Feltham, R. D.; Enemark, J. H. *Top. Inorg. Organomet. Stereochem.* **1981**, *12*, 155.

(7) Bottomley, F. In *Reactions of Coordinated Ligands*; Braterman, P. S., Ed.; Plenum Publishing Corp.: New York, 1989; Vol. 2.

(8) (a) Callahan, R. W.; Meyer, T. J. *Inorg. Chem.* **1977**, *16*, 574−581. (b) Pipes, D. W.; Meyer, T. J. *Inorg. Chem.* **1984**, *23*, 2466−2472.

(9) Roncaroli, F.; Ruggiero, M. E.; Franco, D. W.; Estiú, G. L.; Olabe, J. A. *Inorg. Chem.* **2002**, *41*, 5760−5769.

(10) (a) Lee, C. M.; Chen, C. H.; Chen, H. W.; Hsu, J. L.; Lee, G. H.; Liaw, W. F. *Inorg. Chem.* **2005**, *44*, 6670−6679. (b) Karidi, K.; Garoufis, A.; Tsipis, A.; Hadjiliadis, N.; den Dulk, H.; Reedijk, J. *Dalton Trans*. **2005**, *7*, 1176−1187. (c) Zampieri, R. C. L.; Von Poelhsitz, G.; Batista, A. A.; Nascimento, O. R.; Ellena, J.; Castellano, E. E. *J. Inorg. Biochem.* **2002**, *92*, 82−88. (d) Serli, B.; Zangrando, E.; Iengo, E.; Alessio, E. *Inorg. Chim. Acta* **2002**, *339*, 265−272. (e) Nagao, H.; Hirano, T.; Tsuboya, N.; Shiota, S.; Mukaida, M.; Oi, T.; Yamasaki, M. *Inorg. Chem.* **2002**, *41*, 6267−6273. (f) Grapperhaus, C. A.; Patra, A. K.; Mashuta, M. S. *Inorg. Chem.* **2002**, *41*, 1039−1041. (g) Hadadzadeh, H.; DeRosa, M. C.; Yap, G. P. A.; Rezvani, A. R.; Crutchley, R. J. *Inorg. Chem.* **2002**, *41*, 6521−6526. (h) Batista, A. A.; Queiroz, S. L.; Healy, P. C.; Bucley, R. W.; Boyd, S. E.; Berners-Price, S. J.; Castellano, E. E.; Ellena, J. *Can. J. Chem.* **2001**, *79*, 1030−1035. (i) Ray, M.; Golombek, A. P.; Hendrich, M. P.; Yap, G. P. A.; Liable-Sands, L. M.; Rheingold, A. L.; Borovik, A. S. *Inorg. Chem.* **1999**, *38*, 3110−3115. (j) Schweitzer, D.; Ellison, J. J.; Shoner, S. C.; Lovell, S.; Kovacs, J. A. *J. Am. Chem. Soc.* **1996**, *118*, 10996−10997. (k) Ooyama, D.; Miura, Y.; Kanazawa (Kitanaka), Y.; Howell, F. S.; Nagao, N.; Mukaida, M.; Nagao, H.; Tanaka, K. *Inorg. Chim. Acta* **1995**, *237*, 47−55. (l) Coe, B. J.; Chery, M.; Beddoes, R. L.; Hope, H.; White, P. S. *J. Chem. Soc., Dalton Trans*. **1996**, 3917. (m) Togano, T.; Kuroda, H.; Nagao, N.; Maekawa, Y.; Nishimura, H.; Howell, F. S.; Mukaida, M. *Inorg. Chim. Acta* **1992**, *196*, 57−63. (n) Szczepura, L. F.; Muller, J. G.; Bessel, C. A.; See, R. F.; Janik, T. S.; Churchill, M. R.; Takeuchi, K. J. *Inorg. Chem.* **1992**, *31*, 859−869. (o) Nagao, H.; Nishimura, H.; Funato, H.; Ichikawa, Y.; Howell, F. S.; Mukaida, M.; Kakihana, H. *Inorg. Chem.* **1989**, *28*, 3955−3959. (p) Zanichelli, P. G.; Miotto, A. M.; Estrela, H. F. G.; Rocha Soares, F.; Grassi-Kassisse, D. M.; Spadari-Bratfisch, R. C.; Castellano, E. E.; Roncaroli, F.; Parise, A. R.; Olabe, J. A.; de Brito, A. R. M. S.; Franco, D. W. *J. Inorg. Biochem.* **2004**, *98*, 1921−1932. (q) Lang, R. D.; Davis, J. A.; Lopez, L. G. F.; Ferro, A. A.; Vasconcellos, L. C. G.; Franco, D. W.; Tfouni, E.; Wieraszko, A.; Clarke, M. J. *Inorg. Chem.* **2000**, *39*, 2294−2300. (r) Sauaia, M. G.; Oliveira, F. d. S.; Lima, R. G. d.; Cacciari, A. d. L.; Tfouni, E.; Santana da Silva, R. *Inorg. Chem. Commun.* **2005**, *8*, 347−349. (s) Pitarch López, J.; Heinemman, F. W.; Prakash, R.; Hess, B. A.; Horner, O.; Jeandey, C.; Oddou, J. L.; Latour, J. M.; Grohmann, A. *Chem.−Eur. J.* **2002**, *8*, 5709−5722. (t) de Souza, V. R.; de Costa Ferreira, A. M.; Toma, H. E. *Dalton. Trans.* **2003**, 458−463.

(11) (a) Patra, A. K.; Rose, M. J.; Murphy, K. A.; Olmstead, M. M.; Mascharak, P. K. *Inorg. Chem.* **2004**, *43*, 4487−4495. (b) Patra, A. K.; Mascharak, P. K. **2003**, *42*, 7363−7365. (c) Afshar, R. K.; Patra, A. K.; Bill, E.; Olmstead, M. M.; Mascharak, P. K. *Inorg. Chem.* **2006**, *45*, 3774−3781.

(12) (a) Sarkar, S.; Sarkar, B.; Chanda, N.; Kar, S.; Mobin, S. M.; Fiedler, J.; Kaim, W.; Lahiri, G. K. *Inorg. Chem.* **2005**, *44*, 6092−6099. (b) Chanda, N.; Paul, D.; Kar, S.; Mobin, S. M.; Datta, A.; Puranik, V. G.; Rao, K. K.; Lahiri, G. K. *Inorg. Chem.* **2005**, *44*, 3499−3511. (c) Chanda, N.; Mobin, S. M.; Puranik, V. G.; Datta, A.; Niemeyer, M.; Lahiri, G. K. *Inorg. Chem.* **2004**, *43*, 1056−1064. (d) Mondal, B.; Paul, H.; Puranik, V. G.; Lahiri, G. K. *J. Chem. Soc., Dalton Trans.* **2001**, 481−487.

(13) Pettinari, C.; Santini, C. *Polypyrazolylborate and Scorpionate Ligands*; Elsevier: Oxford, U.K., 2004; Vol. 1, Chapter 1.10.

(14) Bigmore, H. L.; Lawrence, S. C.; Mountford, P.; Tradget, C. S. *Dalton Trans.* **2005**, 635−651.

(15) Astley, T.; Gulbis, J. M.; Hitchman, M. A.; Tiekink, E. R. T. *J. Chem. Soc., Dalton Trans.* **1993**, 509−515.

(16) (a) Trofimenko, S. *Chem. Rev.* **1993**, *93*, 943−980. (b) Trofimenko, S. *J. Am. Chem. Soc.* **1970**, *92*, 5118−5126.

with both fundamental and bioinorganic relevance, envisaged as a pioneering approach in order to deal systematically with the factors influencing this type of reactivity.

Experimental Section

Materials and Reagents. The reagents employed in the synthetic procedures were purchased from Aldrich or Merck and used without further purification. $Eu(NO_3)_3 \cdot 6H_2O$ (>99%) was purchased from Fluka. This compound was reduced with Zn(Hg) in order to generate solutions of Eu^{2+} (1.7×10^{-3} M in 0.1 M $HClO_4$). Dioxygen (O_2; 99.5%) was purchased from Air Liquide. All of the organic solvents employed in synthetic procedures or physical determinations were dried and freshly distilled before use, following standard procedures. A vacuum line and Schlenk glassware were employed when the manipulation required exclusion of air.

Synthesis of Compounds. The syntheses of the tpm ligand and the precursor complex $Ru(tpm)Cl_3$ were performed as described in the literature.[14,18,19] The inclusion of the bpy ligand in the coordination sphere of the latter species to yield $[Ru(bpy)(tpm)Cl]^+$ and its subsequent conversion to $[Ru(bpy)(tpm)H_2O]^{2+}$ were performed by slight modifications of the previously published procedures.[19] We include a detailed description as Supporting Information (SI 1) for completeness.

$[Ru(bpy)(tpm)NO_2](ClO_4)$. A total of 130 mg of $[Ru(bpy)(tpm)H_2O](ClO_4)_2$ (0.19 mmol) and 150 mg of $NaNO_2$ (2.17 mmol) were suspended in 20 mL of water. The mixture was refluxed for 2.5 h under Ar. Cooling in an ice bath precipitated a brilliant-red solid that was collected by filtration, washed with 1−2 mL of chilled water, and dried under vacuum. Yield: 91 mg (76%). Anal. Calcd for $C_{20}H_{18}N_9ClO_6Ru$: C, 38.9; H, 2.9; N, 20.4; O, 15.6. Found: C, 38.6; H, 3.0; N, 19.4; O, 14.4. IR modes for the Ru−NO_2 moiety: ν_{asym}, 1340 cm^{-1}; ν_{sym}, 1304 cm^{-1} (stretchings); δ_{ONO}, 862 cm^{-1}; $\rho_{w(NO_2)}$, 622 cm^{-1}. Electronic absorption spectrum in MeCN: λ_{max}/nm (log ϵ): 476 (3.08), 420 (3.29), 330 sh (3.67), 288 (4.12). CV (MeCN): $E^\circ = 1.13$ V. ^{1}H NMR (MeCN-d_3): δ 8.92 (s, 1H, H_δ), 8.68 (d, 2H, $J_{ab} = 5.4$ Hz, H_a), 8.48 (d, 2H, $J_{cd} = 8$ Hz, H_d), 8.41 (d, 2H, $J_{\beta\gamma} = 2$ Hz, H_γ), 8.39 (d, 2H, $J_{\alpha\beta} = 2.7$ Hz, H_α), 8.30 (d, 1H, $J_{\alpha'\beta'} = 2.7$ Hz, $H_{\alpha'}$), 8.08 (t of d, 2H, $J_{bc} = J_{cd} = 8$ Hz, $J_{ac} = 1.3$ Hz, H_c), 7.51 (d of d of d partially overlapped, 2H, $J_{ab} = 5.4$ Hz, $J_{bc} = 8$ Hz, $J_{bd} = 1.3$ Hz, H_b), 6.68 (m, 3H including $J_{\alpha\beta} = 2.7$ Hz, $J_{\beta\gamma} = 2$ Hz, $J_{\beta'\gamma'} = 2.7$ Hz, H_β, $H_{\gamma'}$), 6.28 (t, 1H, $J_{\alpha'\beta'} = J_{\beta'\gamma'} = 2.7$ Hz, $H_{\beta'}$).

$[Ru(bpy)(tpm)NO](ClO_4)_3 \cdot 0.5H_2O$. A total of 75 mg of $[Ru(bpy)(tpm)NO_2](ClO_4)$ (0.13 mmol) was dissolved in 1 mL of MeCN and 3 mL of 6 M $HClO_4$, with constant stirring, in an ice bath. After 20 min, a pale-yellow precipitate was obtained (2 mL of a saturated solution of $NaClO_4$ was added to favor precipitation). The solid was filtered off, washed with 1−2 mL of chilled water, and dried under vacuum. Yield: 76 mg (77%). Anal. Calcd for $C_{20}H_{19}N_9ClO_{13.5}Ru$: C, 29.7; H, 2.4; N, 15.6; O, 26.7. Found: C, 29.8; H, 2.3; N, 14.8; O, 27.8. IR stretching: $\nu_{NO} = 1959$ cm^{-1} (KBr). Electronic absorption spectrum in MeCN: λ_{max}/nm (log ϵ): 330 sh (3.67), 304 (4.1). CV (MeCN): $E^\circ = 0.65$ V. CV (aqueous, pH 1): $E^\circ = 0.31$ V. ^{1}H NMR (MeCN-d_3): δ 9.49 (s, 1H, H_δ), 8.84 (d(d), 2H, $J_{cd} = 8.1$ Hz, $J_{bd} \sim 1$ Hz, H_d), 8.73 (d, 2H, $J = 2.7$ Hz, H_α or H_γ), 8.66 (d, 2H, $J = 2.4$ Hz, H_α or H_γ), 8.64 (t of d, 2H, $J_{ab} = 7.7$ Hz, $J_{bc} = 7$ Hz, $J_{bd} \sim 1$ Hz, H_b), 8.61 (d(d), 2H, $J_{ab} = 7.7$ Hz, $J_{ac} \sim 1$ Hz, H_a), 8.60 (d, 1H, $J_{\alpha'\beta'} = 2.4$ Hz, $H_{\alpha'}$), 7.94 (d of d of d partially overlapped, 2H, $J_{bc} = 7$ Hz, $J_{cd} = 8.1$ Hz, $J_{ac} \sim 1$ Hz, H_c), 7.03 (d, 1H, $J_{\beta'\gamma'} = 2.7$ Hz, $H_{\gamma'}$), 6.96 (~t, $J_{\alpha\beta}$, $J_{\beta\gamma}$, H_β), 6.49 (~t, $J_{\alpha'\beta'}$, $J_{\beta'\gamma'}$, $H_{\beta'}$).

Instrumentation and Characterization Procedures. Microanalytical data for C, H, N, and O were obtained with a Carlo Erba EA 1108 analyzer. UV−vis spectra were recorded with either an HP8453 or an HP8452A diode array spectrometer. IR spectral measurements were carried out using alternatively one of two Fourier transform spectrophotometers, a Nicolet 150P and a Thermo Nicolet AVATAR 320. Spectra were collected from KBr disks or from solutions in dry MeCN ($CaCl_2$ windows, ∅ = 3 cm, 0.1-mm spacer). The samples were prepared in a drybox (MBraun, Lab master 130). The ^{1}H NMR spectra were measured with a 500-MHz Bruker AM 500 spectrometer; chemical shifts are referred to tetramethylsilane. For electron paramagnetic resonance (EPR), a solution of **I** in MeCN/0.1 M Bu_4NPF_6 was reductively electrolyzed for 5 min at room temperature in a two-electrode capillary cell described elsewhere,[20] leading to a solution of **II**. The spectrum was obtained in a glassy frozen solution at 110 K, with a Bruker ESP 300 spectrometer, equipped with a Bruker ER 35M gaussmeter and an HP5350B microwave counter. The spectral simulations were performed using ad hoc techniques available in Buenos Aires, Argentina. Cyclic voltammetry (CV) and square-wave voltammetry measurements were done in aqueous 0.1 M $HClO_4$ or in MeCN medium (0.1 M Bu_4NPF_6 as the supporting electrolyte) with a standard three-electrode cell containing a Pt working electrode (1.5 mm ∅) or a vitreous C electrode (3 mm ∅) and a Pt wire as the counter electrode. As a reference in aqueous media, a commercial Ag/AgCl (BAS) electrode was used. In MeCN, a Ag wire with either ferrocene or $Ru(bpy)_3^{2+}$ as the internal standard was used. The potential of the working electrode was controlled with one of two commercial potentiostats (Princeton Applied Research 273A or TEQ-03). The spectroelectrochemical experiments in the UV−vis region were done in a homemade cell containing a quartz cuvette (1 cm path), Pt as the working and counter electrodes, and a commercially adapted Ag/AgCl reference electrode. The potential was controlled with a TEQ-03 potentiostat, using 0.1 M $HClO_4$ as the supporting electrolyte. The system was maintained at 25 ± 0.1 °C (RC6 LAUDA thermostat) and was entirely purged with N_2. Throughout this work, all of the reported redox potentials are referred to Ag/AgCl, 3 M NaCl (0.21 V vs NHE).

Crystal Structure Determination. Single crystals of $[Ru(bpy)(tpm)NO](ClO_4)_3$ were obtained by dissolution of $[Ru(bpy)(tpm)NO](ClO_4)_3 \cdot 0.5H_2O$ in MeCN, by adding 1 drop of 1 M $HClO_4$ and slowly diffusing ethyl ether, at room temperature. A small needle-shaped orange crystal was glued on a glass fiber and mounted on a Bruker CCD diffractometer. Data collection was

(17) (a) Serres, R. G.; Grapperhaus, C. A.; Bothe, E.; Bill, E.; Weyhermuller, T.; Neese, F.; Wieghardt, K. *J. Am. Chem. Soc.* **2004**, *126*, 5138−5153. (b) Wanat, A.; Schneppensieper, T.; Stochel, G.; van Eldik, R.; Bill, E.; Wieghardt, K. *Inorg. Chem.* **2002**, *41*, 4−10. (c) Li, M.; Bonnet, D.; Bill, E.; Neese, F.; Weyhermuller, T.; Blum, N.; Sellmann, D.; Wieghardt, K. *Inorg. Chem.* **2002**, *41*, 3444−3456. (d) Brown, C. A.; Pavlosky, M. A.; Westre, T. E.; Zhang, Y.; Hedman, B.; Hodgson, K. O.; Solomon, E. I. *J. Am. Chem. Soc.* **1995**, *117*, 715−732. (e) Westre, T. E.; Di Cicco, A.; Filipponi, A.; Natoli, C. R.; Hedman, B.; Solomon, E. I.; Hodgson, K. O. *J. Am. Chem. Soc.* **1994**, *116*, 6757−6768. (f) Sellmann, D.; Blum, N.; Heinemann, F. W.; Hess, B. A. *Chem.—Eur. J.* **2001**, *7*, 1874−1879. (g) Wanner, M.; Scheiring, T.; Kaim, W.; Slep, L. D.; Baraldo, L. M.; Olabe, J. A.; Zalis, S.; Baerends, E. J. *Inorg. Chem.* **2001**, *40*, 5704−5707. (h) Singh, P.; Sarkar, B.; Sieger, M.; Niemeyer, M.; Fiedler, J.; Zalis, S.; Kaim, W. *Inorg. Chem.* **2006**, *45*, 4602−4609.

(18) (a) Hückel, W.; Bretschneider, H. *Chem. Ber.* **1937**, *9*, 2024−2026. (b) Reger, D. L.; Grattan, T. C.; Brown, K. J.; Little, C. A.; Lamba, J. J. S.; Rheingold, A. L.; Sommer, R. D. *J. Organomet. Chem.* **2000**, *607*, 120−128.

(19) Llobet, A.; Doppelt, P.; Meyer, T. J. *Inorg. Chem.* **1988**, *27*, 514−520.

(20) Frantz, S.; Sarkar, B.; Sieger, M.; Kaim, W.; Roncaroli, F.; Olabe, J. A.; Zalis, S. *Eur. J. Inorg. Chem.* **2004**, 2902−2907.

carried out with the program *SMART-NT*.[21] Data reduction was performed with the program *SAINT-NT*,[21] and a multiscan absorption correction was applied.[21] The structure was solved by direct methods and refined by least squares on F^2.[21] Despite the good appearance of the crystals, the diffracting behavior was poor, mainly because of severe disorder in the anions, to the extent that only one of them could be completely solved. To be able to refine the structure, the other two anions were introduced in the model much in the same way as they appeared in the Fourier map, like two blurred images of perchlorate ions. The only restraint applied was that in each group the most important peaks should determine a Cl atom, while the smaller ones should account for the other four O atoms required for completing each anion. The strategy employed allowed, although poorly, one to refine the whole structure down to a discrepancy factor R1 = 0.157 and, therefore, to extract information on the ordered cation. Because of the data quality, only the Ru center was refined with anisotropic displacement parameters, while the rest were left isotropic. Additionally, a number of metric restraints on presumably equivalent distances were applied in order to ensure convergence within a meaningful geometry.

Addition Reaction of OH^- to I. Kinetic studies for the above reaction were done under pseudo-first-order conditions, at $I = 1$ M (NaCl). Solutions [50.0 mL, $(2.5-5.5) \times 10^{-5}$ M] of the complex were prepared in 10^{-2} M HCl ($I = 1$ M, NaCl) to avoid decomposition of the nitrosyl. On the other hand, buffer solutions (0.1 M, $I = 1$ M, NaCl) were prepared using H_3PO_4/NaH_2PO_4 (pH 2.5−3), CH_3COOH/CH_3COONa (pH 3.5−6), and NaH_2PO_4/Na_2HPO_4 (pH 6−6.5). The pH was checked after each kinetic run. The solutions were thermostated for 15 min with a Lauda RC6 or RC20 instrument. For the samples where the reaction was sufficiently slow, equal volumes of compound and buffer solutions were mixed in a quartz cuvette of 1-cm path length, with stirring. For the mixtures in which the reaction was completed in less than 5 min, the mixing was achieved by a stopped-flow accessory (RX1000 from Applied Photophysics), linked to the diode array spectrometer, and provided with a quartz cuvette similar to that used before. A global analysis[9] of absorbance vs time in the range 220−600 nm was performed in order to obtain the pseudo-first-order rate constant, k_{obs}. Each experiment was repeated at least three times. Plots of k_{obs} vs $[OH^-]$ and of k_{obs} vs $[OH^-]^2$ allowed us to calculate the second-order rate constant and the equilibrium constant (see the text).[9] A direct determination of the latter was not possible because of the absence of good isosbestic points in the spectra of the nitrosyl and the nitro complexes formed over several hours, probably because of decomposition of the latter complex. Rate constants, k_{OH}, at different temperatures (range 20−40 °C) were obtained at pH 4.9 and employed to estimate the activation parameters (enthalpies and entropies) through an Eyring plot, ln k_{OH} vs $1/T$.

Reaction of II with O_2. Kinetic experiments were carried out by mixing solutions of complex **II** (ca. 2.6×10^{-5} M in deoxygenated 0.1 M $HClO_4$) generated in situ (Eu^{2+} as the reducing agent) with aerated 0.1 M $HClO_4$ containing variable amounts of O_2, obtained by dilution of O_2-saturated solutions. To avoid contamination with air during the manipulation of the samples, the mixtures were prepared inside the stopped-flow accessory. The traces obtained at 25 °C were adjusted to a single-exponential decay, at 258 nm. The reported k_{obs} values are the average of at least three consecutive runs. The second-order rate constant was calculated from the slope of k_{obs} vs $[O_2]$.

Theoretical Calculations. We employed density functional theory (DFT)[22] computations to fully optimize the geometries of cations **I** and **II** in vacuo, without symmetry constraints. The calculations were performed with *Gaussian 03*,[23] at the B3LYP level, employing the LanL2DZ basis set, which proved to be suitable for geometry predictions in coordination compounds containing metals of the second and third rows of transition elements in the Periodic Table.[9,22] We used tight self-consistent-field convergence criteria and default settings in the geometry optimizations. **I** is a closed-shell ion, while **II** has an odd number of electrons. Therefore, restricted and unrestricted approximations of the Kohn−Sham equations were used, respectively. To evaluate the nature of the stationary points found in the optimization procedures, the vibrational frequencies were calculated at the equilibrium geometry. For both **I** and **II**, the absence of negative frequencies confirmed that the optimized geometries correspond to stable configurations in the potential energy surface. A time-dependent (TD)DFT computation at the equilibrium geometry for **I** and **II** was employed as an assistant tool in the interpretation and assignment of the electronic spectra.

Results and Discussion

Synthetic Strategy and Basic Characterization. We managed to prepare the new complex $[Ru(bpy)(tpm)NO](ClO_4)_3$, (**I**)$(ClO_4)_3$, with a $\{Ru-NO\}^6$ six-coordinated trication in good yield, employing a two-step procedure. It involved the conversion of $[Ru(bpy)(tpm)H_2O]^{2+}$ into the nitro compound $[Ru(bpy)(tpm)NO_2]^+$ (presently isolated as the perchlorate salt), followed by reaction of the latter with acid to yield complex **I**, with the bound nitrosyl ligand, in a way that was reported for related systems.[4] It is worth mentioning that it is possible to achieve the in situ conversion of the aqua into the nitrosyl species without the intermediate precipitation of the nitro compound. In our hands, however, this alternative route did not improve the overall yield and required more purification steps.

Identification of the $[Ru(bpy)(tpm)NO]^{3+}$ entity as well as other $[Ru(bpy)(tpm)X]^{n+}$ ions ($X = Cl^-$, H_2O, NO_2^-) can be achieved through the analysis of ^1H NMR spectroscopy. The spectra consist of 11 signals that integrate to 18 protons. Ten of these signals are aromatic (4 from bpy and only 6 from tpm due to magnetic equivalence), with δ values between 6 and 9 ppm. The aliphatic H of the tpm ligand appears to be much more displaced, at δ values between 8.9 and 12.3 ppm, depending on the complex (see SI 2 in the Supporting Information for the assignment codes and spectra).

Crystal Structure. The compound $[Ru(bpy)(tpm)NO](ClO_4)_3$ crystallizes in the space group $P2_12_12_1$, with monomeric $[Ru(bpy)(tpm)NO]^{3+}$ cationic units counterbalanced by three perchlorate ions. The relevant crystallographic information, refinement data for the structure, and some

(21) (a) *SMART. Data Collection Software*, version 5.625; Bruker Analytical X-ray Instruments Inc.: Madison, WI, 2001. (b) *SAINT. Data Reduction Software*, version 6.28A; Bruker Analytical X-ray Instruments Inc.: Madison, WI, 2001. (c) Sheldrick, G. M. *SADABS: A Program for Absorption Correction*; Universität Göttingen: Göttingen, Germany, 1996. (d) Sheldrick, G. M. *SHELXS-97 and SHELXL-97: Programs for Structure Resolution and Refinement*; Universität Göttingen: Göttingen, Germany, 1997.

(22) Li, J.; Noodleman, L.; Case, D. A. Electronic Structure Calculations with Applications to Transition Metal Complexes. In *Inorganic Electronic Structure and Spectroscopy*; Solomon, E. I., Lever, A. B. P., Eds.; Wiley: New York, 1999; Vol. I, pp 661−724.

(23) *Gaussian 03*, revision D.01; Gaussian, Inc.: Wallingford, CT, 2004.

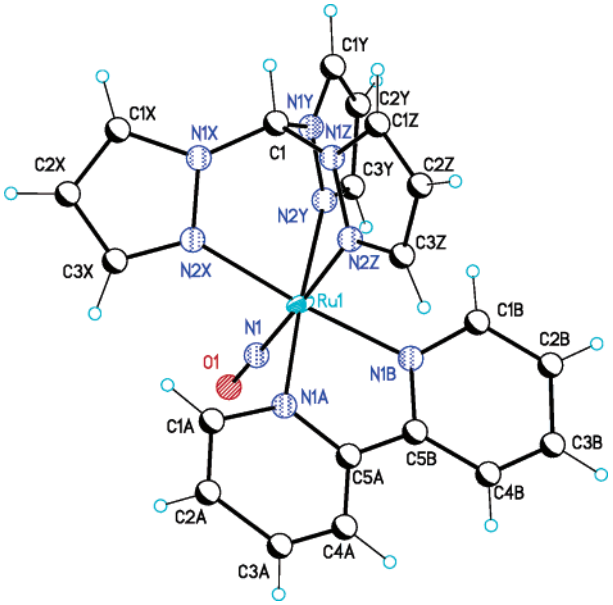

Figure 1. Molecular diagram of the $[Ru(bpy)(tpm)NO]^{3+}$ cation, showing the labeling scheme used. Ru1 refined with an anisotropic displacement factor and drawn at a 30% probability level. The rest, isotropically refined, are drawn as circles of arbitrary radii.

selected distances and angles are shown in SI 3 and SI 4 in the Supporting Information. Figure 1 displays the geometry of the cation, with an appropriate numbering system. The Ru atom is placed in an N_6 environment, generated by the tridentate tpm, the bidentate bpy, and the nitrosyl group, with an average Ru−N distance of 2.009 Å. The N−Ru−N angles deviate from the values expected for a regular octahedron because of the chelating nature of bpy [N1A−Ru−N1B: 77.7(6)°] and of tpm [average N−Ru−N: 83.9(6)°]. At 1.774 Å, the Ru−N1 bond is significantly shorter than the five remaining Ru−N bonds [average Ru−N: 2.023(12) and 2.077(12) Å for bpy and tpm, respectively], a fact that suggests a higher degree of covalency than for the rest of the Ru−N bonds. This value for Ru−N1, the value of 1.09 Å for the N−O distance, and the linear nature of the RuNO moiety (∠Ru−N1−O1: 179.1°) are consistent with the expectations according to the E−F model for a $\{Ru-NO\}^6$ formulation.[5,6]

The DFT-optimized geometry of **I**, shown in SI 5a in the Supporting Information, reproduces the main structural aspects. The Ru−N distances collected in SI 4 of the Supporting Information are, not unexpectedly,[9,22] slightly longer than the experimental ones. The rest of the coordination sphere is reasonably reproduced. The Mayer bond orders confirm the higher degree of covalency for Ru−N1 [0.99 vs 0.29 and 0.48 for Ru−N(tpm) and Ru−N(bpy), respectively]. An orbital analysis shows that the lowest unoccupied molecular orbital (LUMO) and LUMO+1 result from the interaction between the π^* orbitals of the nitrosyl group with $t_{2g}(d_\pi)$ orbitals, leading to ca. 25−30% contribution from the metal center, suggesting a sizable degree of back-donation. The π interaction lowers the energy of the t_{2g} orbitals, leading to filled frontier orbitals that are mostly located on the coligands. As a matter of fact, the highest occupied molecular orbital (HOMO) of the molecule is strongly localized on the bpy ligand, with only marginal contribution from metal orbitals. The latter show up as significant constituents of orbitals as low in energy as HOMO−10, though mixed with bpy- and tpm-centered orbitals.

IR and Electronic Spectra. The IR spectrum of $[Ru(bpy)(tpm)NO](ClO_4)_3 \cdot 0.5H_2O$ in a KBr disk displays a sharp, intense band at 1959 cm^{-1}, assignable to the stretching vibration ν_{NO}.[4] The calculation positions this vibration at a somewhat lower frequency (1881 cm^{-1}) though still in fair agreement (cf. ref 9). The spectrum lacks other informative IR transitions, and most of the signals in the lower energy region arise from C−H stretchings and torsions of the coligands (1200−1600 and 630−860 cm^{-1} for bpy and tpm, respectively),[24] the bands of the perchlorate counterion appear at 1050 and 1150 cm^{-1}. ν_{NO} shifts only slightly when the spectrum is recorded in solution. For instance, ν_{NO} appears at 1962 cm^{-1} in MeCN. The ν_{NO} frequency has been extensively employed to analyze the degree of electronic interaction between the NO ligand and the metal center. Compound **I** shows a very high ν_{NO} value, if compared to related systems reported in the literature,[8−12] indicative of a high nitrosonium (NO^+) character, that is, a $[Ru^{II}NO^+]$ electronic distribution,[4−6] where the NO^+ character is well preserved.

The electronic spectrum of **I** in an aqueous solution does not reveal the typical $d\pi \rightarrow \pi^*(bpy)$ bands observed in other $[Ru(bpy)(tpm)X]^{n+}$ ions ($X = Cl^-$, H_2O, NO_2^-).[25] These transitions are most probably shifted to much higher energy because of the strong π stabilization of the metal d orbitals. The most remarkable spectral features show up at 304 nm (ϵ = 11 000 M^{-1} cm^{-1} in H_2O and 12 600 M^{-1} cm^{-1} in MeCN) with a noticeable shoulder on the low-energy side at 340 nm (ϵ = 3500 M^{-1} cm^{-1}), which slightly shifts to 330 nm (ϵ = 5650 M^{-1} cm^{-1}) when the spectrum is recorded in MeCN. Following TDDFT computational results, these transitions are mostly $\pi \rightarrow \pi^*(bpy)$ in origin. The equivalent intraligand transitions involving tpm appear at higher energy, overlapping with the metal-to-ligand charge-transfer bands $d_\pi \rightarrow \pi^*(bpy)$; both are thus responsible for the high-intensity absorption in the UV region.

{RuNO}[6,7] Interconversion. The cyclic voltammogram of **I** (SI 6 in the Supporting Information) in aqueous solution (pH 1, $HClO_4$, I = 0.1 M) displays a single reversible wave at 0.31 V, arising from the one-electron reduction of **I** to the $\{Ru-NO\}^7$ species $[Ru(bpy)(tpm)NO]^{2+}$ (**II**). In a MeCN solution, the solvent window allowed us to extend the electrochemical exploration into more negative potential regions, leading to the observation of two consecutive one-electron processes at +0.60 V (reversible) and at −0.2 V (irreversible), which could be ascribed to the formation of $\{RuNO\}^7$ and (presumably) a $\{RuNO\}^8$ species or, correspondingly, as the conversion of bound NO^+ into $NO^\bullet$ and NO^- (HNO).[8]

Reversible one-electron processes are common features of many nitrosyl complexes. The $E_{NO^+/NO}$ redox potentials

(24) Nakamoto, K. *Infrared and Raman Spectra of Inorganic and Coordination Compounds*, 4th ed.; Wiley: New York, 1986.
(25) Llobet, A. *Inorg. Chim. Acta* **1994**, *221*, 125−131.

Table 1. Addition Rate Constants, Activation Parameters, and Other Indicators for a Selected Group of Nitrosyl Compounds, $[RuL_5NO]^n$

compound[a]	$k_{OH^-}/(M^{-1}\ s^{-1})$	k_4/s^{-1}	$\Delta H^{\ddagger}/(kJ\ mol^{-1})$	$\Delta S^{\ddagger}/(J\ K^{-1}\ mol^{-1})$	$E_{NO^+/NO}$[b]/V	ν_{NO}/cm^{-1}	K_1/M^{-2}
$[Ru(bpy)(tpm)NO](ClO_4)_3$	3.1×10^6	1.4×10^6	94	193	0.31	1959	4.4×10^{21}
$[Ru(bpy)(trpy)NO](PF_6)_3$	3.2×10^5	1.3×10^5	89	159	0.25	1946	2.1×10^{23}
cis-$[Ru(bpy)_2ClNO](PF_6)_2$	8.5×10^3	4.6×10^3	100	164	0.05	1933	1.6×10^{15}
trans-$[Ru(NH_3)_4pzNO](BF_4)_3$	1.8×10^2	9.6×10^1	76	54	−0.11	1942	6.0×10^8
$Na_2[Ru(CN)_5NO]\cdot 2H_2O$	9.5×10^{-1}	6.4	57	−54	−0.35	1926	4.4×10^6

[a] Data are from ref 9, with the exception of the presently reported tpm complex. [b] vs Ag/AgCl, 3 M NaCl. pH 2.0, except that for the tpm complex, which is pH 1.0.

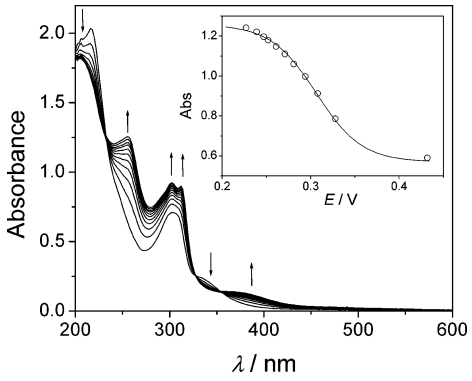

Figure 2. Spectroelectrochemical reduction of **I** into **II** under controlled potential conditions. [complex] = 5.6×10^{-5} M. Inset: Absorbance at 258 nm vs open-circuit potential during electrolysis.

span a broad range and are very sensitive to the σ donor and π acceptor/donor abilities of the coligands present in the coordination sphere (Table 1).[9] As with the ν_{NO} frequencies, redox potentials provide information about the electronic nature of the compound. High redox potentials usually correlate with high NO stretching frequencies and reflect a smaller degree of metal-to-nitrosyl back-bonding. The newly prepared **I** has an even higher redox potential value than the one found for the $[Ru(bpy)(trpy)NO]^{3+}$ ion, 0.25 V, and the same can be said about ν_{NO} (1962 vs 1946 cm^{-1}),[9] suggesting that the Ru center in **I** behaves as a poorer electron donor.

Figure 2 shows the stepwise **I** → **II** conversion under controlled potential conditions in an aqueous solution, pH 1. The reduction proceeds smoothly, showing isosbestic points at 232, 328, and 354 nm. The integrated current, as well as the absorbance vs open-circuit potential curve (Figure 2, inset) obtained during the electrolysis, is also consistent with a one-electron process with $E_{NO^+/NO} = 0.31$ V, in agreement with the CV studies. Even without attempts at a full assignment, some spectral changes deserve a comment. The UV region (maxima at 256, 302, and 312 nm, with ϵ values of 19 500, 14 500, and 14 100 $M^{-1}\ cm^{-1}$, respectively) is comparable to the one for the $\{RuNO\}^6$ species, except for the intensity and minor shifts. The lower energy transition (370 nm, $\epsilon = 2140\ M^{-1}\ cm^{-1}$) is comparable in energy and intensity to the $d\pi \rightarrow \pi^*$(bpy) absorptions already reported in $[Ru(bpy)(tpm)Cl]^+$ and $[Ru(bpy)(tpm)H_2O]^{2+}$.[19] Its occurrence reflects the destabilization of the $d\pi$ orbitals upon reduction of the strong π acceptor NO^+ to the less interacting NO.

There are no spectroscopic signs of decomposition of the reduced species if protected from O_2, and reoxidation leads to quantitative recovery of **I** even after several hours. The reversibility of the NO^+/NO conversion indicates that the whole coordination sphere in **II** (including the coordinated $NO^{\bullet}$) is strongly inert toward substitution reactions. This is not always the case, and there are reports that suggest the possibility of NO-induced trans labilization on the time scale of minutes for several complexes.[4] This appears not to be the case with **II**, making this system particularly useful for study in both $\{RuNO\}^{6,7}$ oxidation states.

The reduction process can also be achieved by chemical means, employing, for instance, $Ru(py)_4Cl_2$ as the reducing agent. Chemical reduction permitted the preparation of concentrated solutions of **II** (ca. 10 mM), used to record the IR spectrum in a MeCN solution. The most relevant spectral change involves the shift of ν_{NO} from 1960 to 1660 cm^{-1}. Such a 300-cm^{-1} decrease of ν_{NO} upon one-electron reduction has been observed for several nitrosyl complexes and is indicative of the population of the MNO antibonding orbital.[8,9,26] The optimized geometry of **II** derived from DFT computations is consistent with this analysis (SI 7 in the Supporting Information). The presence of an extra electron leads to a computed Ru1−N−O angle of 140.3° and a ν_{NO} frequency of 1640 cm^{-1} (see SI 4 in the Supporting Information for other distances and angles). The value of ν_{NO} is very close to the experimentally determined value, while the Ru−N−O bending is consistent with data available for related $\{RuNO\}^7$ complexes.[17] The electronic structure calculations locate the unpaired electron mostly on the NO ligand, with partial delocalization on the metal (Figure 3, inset) The EPR spectroscopy in MeCN at 110 K is consistent with this interpretation. Figure 3 shows an anisotropic signal arising from an $S = {}^1/_2$ electronic ground state, with evidence of coupling of the unpaired electron with the nuclear spin of ^{14}N ($I = 1$, 99.6%). The fitting procedure provided estimates for the main components of the g matrix at 2.031, 1.990, and 1.886 and of the hyperfine coupling tensor with $A/10^{-4}\ cm^{-1} = 9.2$, 31.8, and 1.9 (A_1 and A_3 unresolved). The signal resembles those of spectra reported previously for complexes $\{MNO\}^7$ (M = Fe, Ru, Os).[8,10−12,17,20] The rather high value of A_2 indicates a considerable degree of localization of the unpaired spin in the vicinity of the N nucleus. The deviation of g from the free electron value (2.0023) is due to spin−orbit-induced mixing with excited states with orbital angular momentum, reflecting the partial delocalization of the spin density on Ru, which exhibits a spin−orbit coupling constant of 1200 cm^{-1}. In agreement with these general and unusually invariant EPR features, an

(26) (a) Fiedler, J. *Collect. Czech. Chem. Commun.* **1993**, *58*, 461−473. (b) Baumann, F.; Kaim, W.; Baraldo, L. M.; Slep, L. D.; Olabe, J. A.; Fiedler, J. *Inorg. Chim. Acta* **1999**, *285*, 129−133.

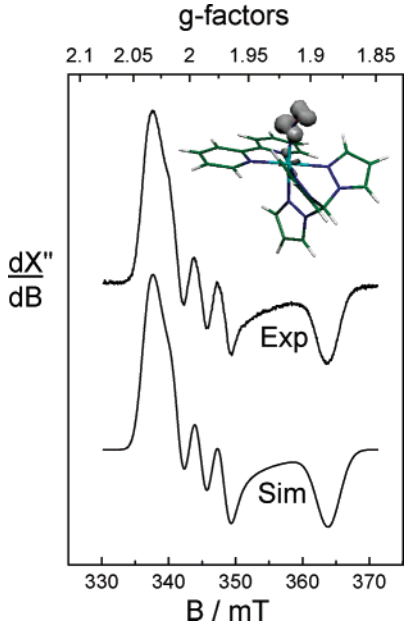

Figure 3. Top right: DFT-calculated spin density of **II** in a vacuum (B3LYP level, LanL2DZ basis set). Middle: EPR spectrum of the electrogenerated cation $[Ru(bpy)(tpm)NO]^{2+}$ (**II**) in MeCN/0.1 M Bu_4NPF_6 at 110 K. Experimental conditions: microwave frequency, 9.604 GHz; modulation amplitude, 4 G. Bottom: Computer-simulated spectrum (see the parameters in the text).

approximate spin distribution with $^2/_3$ on NO and $^1/_3$ on Ru has been established.[20]

Chemical reoxidation of **II** with [tris(4-bromophenyl)-ammoniumyl]hexachloroantimonate leads to complete recovery of **I**. Strikingly enough, reoxidation with O_2 in the absence of water leads to an unidentified intermediate product with bands at 1714 and 1223 cm^{-1}.

Electrophilic Reactivity in Aqueous Solution: Reaction with OH^-. The electrophilic reactivity of $\{M-NO\}^6$ species has been studied for a long time and has been comprehensively reviewed.[2,7,27] The most representative mechanistic analyses deal with the reactions with OH^-, the stoichiometry of which is represented by eq 1. This reaction is particularly suited for systematic studies because it does not exhibit redox decomposition following the primary elementary addition step, as is frequently reported with other N- and S-binding nucleophiles:[7,9]

$$[ML_5NO]^n + 2OH^- \rightarrow [ML_5NO_2]^{n-2} + H_2O \qquad K_1 \qquad (1)$$

Equation 1 is formally an acid−base interconversion, with values of K_1 that depend on the electronic properties of the ML_5 moiety. The equilibrium constant increases with the degree of nitrosonium (NO^+) character of the nitrosyl ligand. The largest reported values correspond to the presence of electron-withdrawing coligands (viz., the polypyridines).[8,9] In these cases, a high $MNO^+ \rightarrow MNO_2^-$ conversion can be achieved even at very low pH values (near 0). On the other hand, weaker electrophiles such as $[Fe(CN)_5NO]^{2-}$ need to attain pH values >10 in order to reach a full conversion to nitrite.[27]

(27) Olabe, J. A. *Adv. Inorg. Chem.* **2004**, *55*, 61−126.

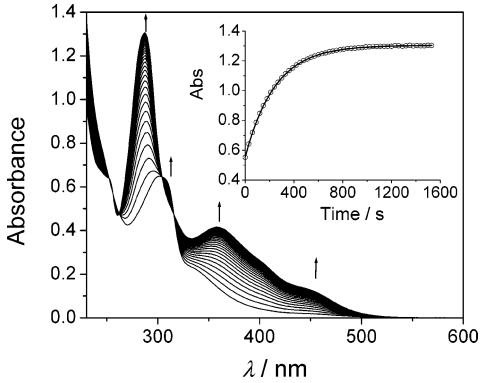

Figure 4. Successive spectra for the reaction of **I** with OH^-. $I = 1$ M (NaCl), $T = 25$ °C, $[OH^-] = 2.2 \times 10^{-9}$ M, and [complex] $= 5.4 \times 10^{-5}$ M. Inset: Absorption increase vs time at 288 nm.

Figure 4 shows the stepwise conversion of $[Ru(bpy)(tpm)NO]^{3+}$ into $[Ru(bpy)(tpm)NO_2]^+$ at a given pH. The spectral features of the final product are identical with those of the nitro precursor, suggesting that the reaction that takes place is

$$[Ru(bpy)(tpm)NO]^{3+} + 2OH^- \rightarrow [Ru(bpy)(tpm)NO_2]^+ + H_2O \qquad K_2 \qquad (2)$$

The reaction with OH^- is reversible, and a full recovery of the nitrosyl reactant can be achieved upon acidification. The presence of well-defined isosbestic points at 262, 304, and 315 nm suggests the absence of processes other than the one described by eq 2. An equimolar mixture of both complexes is attained at a pH of ca. 3.0−3.5. The time required to fully equilibrate the solutions at such acidic pH values is too long; therefore, it precludes an accurate estimation of the equilibrium constant K_2, which must be close to 5×10^{21} M^{-2} anyway.

The use of thermodynamic indicators (affinities or K values for reactions such as eq 1) or of ν_{NO} values has been objected for obtaining a quantitative, predictive estimation of the electrophilicity of nitrosyl.[9] The latter is a kinetic concept, and therefore some mechanistic insight should be obtained for reactions such as eq 1. On the basis of a previously developed analysis,[28] we propose reactions (3)−(5) as a suitable path for reaction (2).

$$[Ru(bpy)(tpm)NO]^{3+} + OH^- \rightarrow [Ru(bpy)(tpm)NO^{3+}\cdot OH^-] \qquad K_{ip3} \qquad (3)$$

$$[Ru(bpy)(tpm)NO^{3+}\cdot OH^-] \rightarrow [Ru(bpy)(tpm)NO_2H]^{2+} \qquad K_4, k_4, k_{-4} \qquad (4)$$

$$[Ru(bpy)(tpm)NO_2H]^{2+} + OH^- \rightarrow [Ru(bpy)(tpm)NO_2]^+ + H_2O \qquad K_5 \qquad (5)$$

Reaction (3) is a fast ion-pair equilibrium step, and the value of K_{ip3} can be estimated in terms of electrostatic models.[9] Reaction (4) is the true nucleophilic addition step,

(28) Baraldo, L. M.; Bessega, M. S.; Rigotti, G. E.; Olabe, J. A. *Inorg. Chem.* **1994**, *33*, 5890−5896.

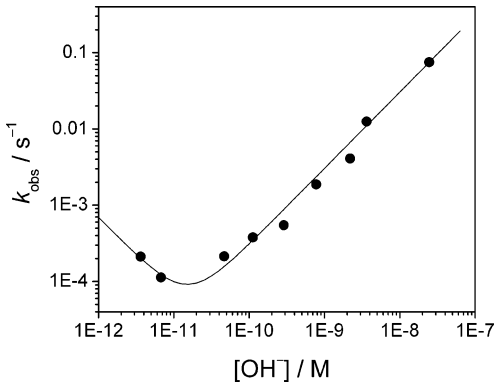

Figure 5. Dependence of k_{obs} on [OH$^-$] for **I**. $I = 1$ M (NaCl), $T = 25$ °C, and [complex] = (2.5−5.5) × 10^{-5} M.

involving the conversion of an outer-sphere complex into an inner-sphere one containing a bound NO_2H intermediate. We should envisage the direct step in reaction (4) as the relevant one for measuring the electrophilicity of bound NO^+, with k_4 as the significant indicator. Finally, deprotonation of the nitrous acid intermediate occurs rapidly, leading to the nitro complex product (eq 5).

The inset of Figure 4 shows a first-order increase of the product absorbance in reaction (2). The rate constants, k_{obs}, have been measured for different concentrations of OH^-, and Figure 5 shows the functional relationship. Assuming a steady-state concentration of the nitrous acid intermediate, the mechanistic treatment leads to

$$k_{obs} = k_{OH}\left\{[OH^-] + \frac{1}{[OH^-]}K_2\right\} \qquad (6)$$

with $k_{OH} = K_{ip3}k_4$ and $K_2 = K_{ip3}K_4K_5$.[9] For sufficiently high values of [OH$^-$], the second term in eq 6 can be neglected and $k_{obs} = k_{OH}$[OH$^-$]. This behavior can be appreciated in Figure 5 (right side), reflecting a first-order behavior in each reactant. The deviations from linearity for low values of [OH$^-$] reflect the contribution of k_{-4}, through the value of K_2 (see above). With the calculated value of K_{ip3}, 2.4 M^{-1}, and through fitting of the proper value of k_{OH} in Figure 5, 3.05 × 10^6 M^{-1} s^{-1}, a value of k_4 can be obtained, 1.26 × 10^6 s^{-1}. By extending the working range toward lower pHs, we estimate $K_2 = 4.4 \times 10^{21}$ M^{-2}.

In Table 1, we show thermodynamic and kinetic parameters for a selected group of {RuNO}^{6} compounds. It can be seen that **I** is placed at the top, with the highest values for k_4, ν_{NO}, and $E_{NO^+/NO}$. A linear-free-energy relationship emerges by plotting ln k_4 against $E_{NO^+/NO}$ for an impressive set of nitrosyl complexes.[9] The activation enthalpies and entropies increase when going upward in the table. For [Ru(bpy)(tpm)NO]$^{3+}$, we found $\Delta H^{\ddagger} = 94$ kJ mol^{-1} and $\Delta S^{\ddagger} =$ 193 J K^{-1} mol^{-1}, comparable to values found for other electron-deficient nitrosyl complexes. The trend in $\Delta H^{\ddagger}$ is governed by the energy required for the angular reorganization process that follows the OH^- coordination, which increases as the positive charge in the nitrosyl-containing moiety becomes larger. The experimental $\Delta S^{\ddagger}$ tendency reflects the solvation effects associated with the charges in the reactants. Because the rate constants increase in parallel with both $\Delta H^{\ddagger}$ and $\Delta S^{\ddagger}$, it has been concluded that these reactions are entropically driven.

In recent years, new complexes of the [Ru(trpy)(L)NO]$^{3+}$ series (trpy = 2,2′:6′,2″-terpyridine), with L = azopyridines, 2,2′-pyridylamine, 2-(2-pyridyl)azoles, and 2,2′-dipyridyl ketone, have been synthesized and characterized.[12] All of the L ligands are strong π acceptors with variable strength (the azopyridine complexes show very high ν_{NO} values), and the overall picture agrees with the presence of nitrosyl groups with high nitrosonium character. Unfortunately, the reported data on the kinetics of the $RuNO^+/RuNO_2^-$ conversions have been obtained in mixed aqueous MeCN media, without control of the pH and ionic strength. The authors have reported k_{obs} values of ca. 10^{-4} s^{-1} corresponding to the formation of the nitro complexes and have assigned these "slow" reactions to the nucleophilic attack of *water* on the bound nitrosyl.[12] By considering OH^- as the true nucleophile and assuming that its concentration is 10^{-7} M, the second-order rate constants can be estimated to be around 10^3-10^5 M^{-1} s^{-1}, a result that stands in reasonable agreement with the presently and previously reported results and interpretation. As a conclusion, we may confirm that the k_4 values for the nucleophilic additions are very good indicators for the electron density at the N atoms of the MNO moieties, showing a sensitive correlation with the values of $E_{NO^+/NO}$. The latter values, rather than ν_{NO}, appear as more appropriate indicators for predicting the subtle electron distribution changes for the different nitrosyl complexes.[9]

Reaction of II toward O_2. There is a surprising lack of detailed kinetic studies on the reactions of complexes with bound $NO^{\bullet}$ toward O_2.[2] For classical coordination compounds, preliminary reports exist on the fast reactions of $NO^{\bullet}$ bound to $[Fe(CN)_5]^{3-}$ and $[Ru(NH_3)_5]^{2+}$.[29] On the other hand, $NO^{\bullet}$ bound to porphyrins or hemoproteins appears to be generally unreactive toward O_2.[1,2,30] There are reports that show slow reaction with O_2, leading to nitrate, as in the case of myoglobin,[31] but these reactions are probably rate-controlled by NO dissociation from the metal, with subsequent O_2 coordination and further reaction.[2] The autoxidation reactions of {MNO}^{7} complexes appear strongly dependent on the coordination number, requiring six-coordination to attain appreciable rates.[32] Besides, the rates appear to depend strongly on the solvent.[33] The bioinorganic relevance of $NO^{\bullet}$ autoxidation reactions has been addressed mainly in terms of the reactivity of *free* NO.[1,2] This reaction is second- and first-order with respect to NO and O_2, respectively, and leads to nitrite in an aqueous solution. Ambiguities still exist on

(29) (a) Cheney, R. P.; Simic, M. G.; Hoffman, M. Z.; Taub, I. A.; Asmus, K. D. *Inorg. Chem.* **1977**, *16*, 2187−2192. (b) Armor, N. J.; Hoffman, M. Z. *Inorg. Chem.* **1975**, *14*, 444−446.
(30) Hoshino, M.; Laverman, L.; Ford, P. C. *Coord. Chem. Rev.* **1999**, *187*, 75−102.
(31) Andersen, H. J.; Skibsted, L. H. *J. Agric. Food Chem.* **1992**, *40*, 1741−1750.
(32) (a) Patra, A. K.; Rowland, J. M.; Marlin, D. S.; Bill, E.; Olmstead, M. M.; Mascharak, P. K. *Inorg. Chem.* **2003**, *42*, 6812−6823. (b) Cheng, L.; Powell, D. R.; Khan, M. A.; Richter Addo, G. B. *Chem. Commun.* **2000**, 2301.
(33) Harrop, T. C.; Olmstead, M. M.; Mascharak, P. K. *Inorg. Chem.* **2005**, *44*, 6918−6920.

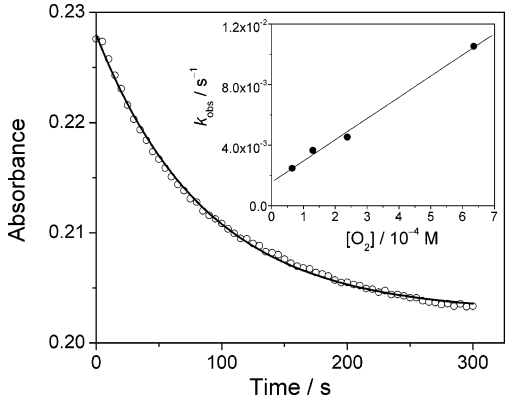

Figure 6. Kinetic trace at 258 nm. [complex] = ca. 2.6×10^{-5} M, and [O_2] = 6.4×10^{-4} M. Inset: Dependence of k_{obs} on [O_2]. I = 0.1 M ($HClO_4$), and T = 25 °C.

the detailed nature of the relevant intermediates.[34] Given the presence of metal ions in bodily fluids, the need for investigating the factors controlling metal-bound NO reactivity is obvious. We considered it useful to obtain some preliminary information on this reaction type using complex **II**.

As stated above, **II** is stable for hours if maintained in an anaerobic medium. However, a conversion to **I** is operative on the time scale of minutes in the presence of air, in an aqueous solution at pH 1. Figure 6 shows a monoexponential decaying trace, measured at 258 nm, under an excess of O_2 over **II**. We propose eq 7 as representative of the overall stoichiometry, based on related measurements performed for the autoxidation reaction of $[Fe(CN)_5NO^{\bullet}]^{3-}$.[35]

$$4[Ru(bpy)(tpm)NO^{\bullet}]^{2+} + O_2 + 4H^+ \rightarrow 4[Ru(bpy)(tpm)NO]^{3+} + 2H_2O \quad (7)$$

The inset in Figure 6 shows a plot with the values of k_{obs} obtained from the pseudo-first-order experiments against the concentration of O_2. The linear behavior sustains the following rate law: $-{}^1/_4\ d[Ru(bpy)(tpm)NO^{2+}]/dt = k_7[Ru(bpy)(tpm)NO^{2+}][O_2]$, with $k_7 = 3.5 \pm 0.2\ M^{-1}\ s^{-1}$ (25 °C).

Given the preliminary character of these results, we avoid speculations on the detailed mechanism, which probably implies an initial adduct formation between O_2 and bound $NO^{\bullet}$.[34,35] In the same way, the value of k_7 does not have much significance per se, unless we recognize that the same rate law has been observed for the autoxidation reactions of the pentacyanoferrate- and pentaamminruthenium complexes of $NO^{\bullet}$, affording second-order rate constants of ca. $10^5-10^6\ M^{-1}\ s^{-1}$.[29,35] The difference of 5−6 orders of magnitude between the values of these rate constants and the presently reported one calls our attention to the probable significance of the $E_{NO^+/NO}$ values in determining the autoxidation rates. In comparison with 0.31 V for $[Ru(bpy)(tpm)NO]^{3+}$, values of $E_{NO^+/NO}$ of around −0.3 V have been reported for $[Fe(CN)_5NO]^{2-}$ and $[Ru(NH_3)_5NO]^{3+}$.[29] These results are not unexpected because the faster reactions occur with the more reductant nitrosyls. A correlation emerges, although with an *opposite slope*, similar to the one found for ln k_4 vs $E_{NO^+/NO}$.[9] Certainly, the possibility of also using the $E_{NO^+/NO}$ values as predictors of the *nucleophilic* reactivity of NO complexes seems attractive. Kinetic work on additional complexes with intermediate $E_{NO^+/NO}$ values is currently underway in order to check the above correlation.

Conclusions

The new ruthenium nitrosyl complex containing tpm and bpy as coligands, $[Ru(bpy)(tpm)NO]^{3+}$ (**I**), exhibits qualitatively the structural and spectroscopic features typical of complexes with the $\{RuNO\}^6$ configuration. Remarkably, however, the very high values of ν_{NO} and $E_{NO^+/NO}$ identify **I** as a strongly electrophilic species, with the nitrosyl group acquiring a high degree of nitrosonium character. This is confirmed by the value of k_{OH}, the nucleophilic rate constant for OH^- addition, *the highest ever* observed for this nucleophile in such a situation. The mechanistic study of the latter reaction highlights the importance of $E_{NO^+/NO}$ values in predicting and controlling the nucleophilic rates for a vast number of $\{RuNO\}^6$ complexes. Complex **I** may be reduced reversibly to the EPR-active $[Ru(bpy)(tpm)NO^{\bullet}]^{2+}$ (**II**) with significant changes in the calculated structural and measured spectroscopic (IR and UV−vis) properties. Noticeably, **II** is a very robust complex toward ligand dissociation. Although some predictable elongation of the Ru−N(O) distance in **II** (1.92 A) compared to **I** (1.77 A) is obtained from the calculations, **II** remains stable for hours in air-free solutions, suggesting a very small NO-dissociation rate constant. However, O_2 allows for reoxidation of **II** to **I**, with a measured second-order rate constant ($3.5\ M^{-1}\ s^{-1}$) significantly smaller than values observed for other M−$NO^{\bullet}$ fragments with lower values of $E_{NO^+/NO}$. This pioneering kinetic approach to the autoxidation reaction of bound $NO^{\bullet}$ has an obvious bioinorganic relevance, given the well-studied but still mechanistically uncertain reactivity of free NO. The demonstrated stabilization of the NO radical complex state can be attributed to the high total charge and to the geometrical and electronic structure as determined largely by the neutral tpm ligand. As the long Ru−N(tpm) bonds attest, this tridentate chelate ligand imposes a certain distortion on the coordination geometry while acting as a weak overall donor.

Acknowledgment. We thank Universidad de Buenos Aires (UBA), the National Scientific Council (CONICET), and the Agency for Science Promotion (ANPCyT) for financial support. M.V. and J.S.J. were graduate and student fellows from CONICET and UBA, respectively. L.D.S. and J.A.O. are members of the research staff of CONICET. P.S. and W.K. thank the Graduate College on Magnetic Resonance of the Deutsche Forschungsgemeinschaft. We also thank Prof. Antoni Llobet for calling our attention to the properties of the tpm ligand.

(34) (a) Goldstein, S.; Czapski, G. *J. Am. Chem. Soc.* **1995**, *117*, 12078−12084. (b) Bohle, D. S. *Curr. Opin. Chem. Biol.* **1998**, *2*, 194−200.
(35) Videla, M.; Roncaroli, F.; Jacinto, J. S.; Slep, L. D.; Olabe, J. A., to be submitted.

Supporting Information Available: SI 1 describes the preparation of compounds containing the $[Ru(tpm)(bpy)X]^{n+}$ ($X = Cl^-$, H_2O) ions. SI 2 shows the ^1H NMR spectra of tpm and the $[Ru(tpm)(bpy)X]^{n+}$ ions ($X = Cl^-$, H_2O, NO_2^-, NO^+). SI 3 and 4 show tables with crystal data and structure refinement for the pechlorate salt of **I** and selected distances and angles, respectively. Parts a and b of SI 5 show the DFT-calculated geometries for complexes **I** and **II**. SI 6 shows the cyclic voltammograms of complex **I**, in aqueous and MeCN solutions. SI 7 shows selected DFT-calculated distances and angles for complex **II**. This material is available free of charge via the Internet at http://pubs.acs.org.

IC061062E